HHS Public Access

Author manuscript

J Invest Dermatol. Author manuscript; available in PMC 2013 October 01.

Published in final edited form as:

J Invest Dermatol. 2013 April ; 133(4): 1043–1051. doi:10.1038/jid.2012.401.

Familial melanoma-associated mutations in p16 uncouple its tumor suppressor functions

Noah C. Jenkins[2,3], **Jae Jung**[1], **Tong Liu**[3], **Megan Wilde**[3], **Sheri L. Holmen**[2,3], and **Douglas Grossman**[1,2,3]

[1]Department of Dermatology, University of Utah Health Sciences Center, Salt Lake City, UT 84112

[2]Department of Oncological Sciences, University of Utah Health Sciences Center, Salt Lake City, UT 84112

[3]Huntsman Cancer Institute, University of Utah Health Sciences Center, Salt Lake City, UT 84112

Abstract

Familial melanoma is associated with point mutations in the cyclin-dependent kinase (CDK) inhibitor $p16^{INK4A}$ (p16). We recently reported that p16 regulates intracellular oxidative stress in a cell cycle-independent manner. Here, we constructed 12 different familial melanoma-associated point mutants spanning the p16 coding region and analyzed their capacity to regulate cell-cycle phase and suppress reactive oxygen species (ROS). Compared to wild-type p16 which fully restored both functions in p16-deficient fibroblasts, various p16 mutants differed in their capacity to normalize ROS and cell cycle profiles. While some mutations did not impair either function, others impaired both. Interestingly, several impaired cell-cycle (R24Q, R99P, V126D) or oxidative function (A36P, A57V, P114S) selectively, indicating that these two functions of p16 can be uncoupled. Similar activities were confirmed with selected mutants in human melanoma cells. Many mutations impairing both cell-cycle and oxidative functions, or only cell cycle function, localize to the third ankyrin repeat of the p16 molecule. Alternatively, most mutations impairing oxidative but not cell-cycle function, or those not impairing either function, lie outside this region. These results demonstrate that particular familial melanoma-associated mutations in p16 can selectively compromise these two independent tumor-suppressor functions, which may be mediated by distinct regions of the protein.

Keywords

p16; melanoma; oxidative stress; cell cycle

Correspondence to: Doug Grossman, MD, PhD at Huntsman Cancer Institute, 2000 Circle of Hope, Suite 5262, Salt Lake City, UT 84112. Phone: 801-581-4682; doug.grossman@hci.utah.edu.

CONFLICT OF INTEREST

The authors have no conflicts of interest to declare.

SUPPLEMENTARY MATERIAL

Supplementary information is available at the JID website.

INTRODUCTION

The CDK4/6 inhibitor $p16^{INK4a}$ (or p16) is encoded by the chromosomal locus *CDKN2A* and altered in most human tumors (Sharpless and DePinho 1999). Germ-line mutations in p16 have been associated more commonly with a subset of cancers, namely pancreatic carcinoma and melanoma, and are inherited in approximately 40% of melanoma-prone families (Goldstein *et al.*, 2007). In the presence of potentially oncogenic stress such as DNA damage, the canonical tumor-suppressor function of p16 involves binding either to cyclin-dependent kinases 4 and/or 6 (CDK4/6) or preassembled CDK4/6-cyclin D complexes (Hirai *et al.*, 1995; Serrano *et al.*, 1993), inhibiting hyperphosphorylation of Retinoblastoma-associated pocket proteins and delaying cell cycle progression from the G1 to S phase (Alcorta *et al.*, 1996; Lukas *et al.*, 1995). In this setting, p16 may induce cellular senescence or allow time for DNA repair prior to cell division (Shapiro *et al.*, 1998). Interestingly, several studies have demonstrated that many familial melanoma-associated p16 mutants retain CDK4-binding capacity *in vitro* (Becker *et al.*, 2001; Hashemi *et al.*, 2000; Kannengiesser *et al.*, 2009; McKenzie *et al.*, 2010), suggesting that p16 may mediate an additional important function(s) independent of cell-cycle regulation.

Since penetrance of melanoma in *p16* mutant kindreds is highly associated with chronic exposure to ultraviolet radiation (Bishop *et al.*, 2002), which produces reactive oxygen species (ROS) in the skin (Herrling *et al.*, 2006), we recently investigated a possible role for p16 in regulating intracellular oxidative stress. We found increased oxidative stress in cells depleted of p16 that was independent of cell-cycle regulation (Jenkins *et al.*, 2011). Melanocytes demonstrated increased susceptibility to oxidative stress in the context of p16 depletion compared to keratinocytes and fibroblasts (Jenkins *et al.*, 2011). Melanocytes thus appear to be more dependent on p16 for normal oxidative regulation than other cell types, which may in part explain why inherited mutations in *p16* predispose to melanoma over other cancers.

Given this newly identified role of p16 in regulating intracellular oxidative stress, we investigated whether different familial melanoma-associated p16 mutations can differentially modulate its cell cycle and oxidative regulatory functions. A panel of p16 mutants was constructed and compared to wild-type p16 in functional assays using $p16^{-/-}Arf^{+/+}$ cells. Interestingly, several mutations selectively compromised control of cell-cycle or oxidative stress, effectively uncoupling these two functions. Taken together, these data show that these two potential tumor-suppressor functions of p16 can be independently disrupted by distinct familial melanoma-associated mutations, and different regions of the protein may be important for these separate functions.

RESULTS

Wild-type p16 suppresses ROS and cell cycle progression, and induces senescence in $p16^{-/-}$ $Arf^{+/+}$ cells

Our previous work (Jenkins *et al.*, 2011) demonstrating sufficiency of p16 in mediating control of intracellular oxidative stress was performed in fibroblasts deficient in *CDKN2A*, which encodes both the p16 and Alternative reading frame (Arf, p19) proteins (Sharpless

and DePinho 1999). We began by confirming these results using cells that were selectively deficient in p16 (i.e. wild-type for Arf). Fibroblasts from wild-type mice were infected with control lentivirus expressing green fluorescent protein (GFP), while $p16^{-/-}Arf^{+/+}$ fibroblasts were separately infected with either lentivirus expressing p16 and GFP or GFP alone. We had previously optimized conditions for viral transduction to achieve 80–90% infection rates (as measured by GFP visualization using fluorescence microscopy) and expression of exogenous p16 (by Western blotting) roughly equivalent to p16 levels in wild-type fibroblasts. Infection of p16-deficient cells with p16 lentivirus resulted in p16 levels comparable to that observed in wild-type cells (Figure 1a, bottom), and was associated with normalization of ROS while ROS levels were significantly higher in p16-deficient cells infected with GFP lentivirus (Figure 1a, top). These control (GFP) $p16^{-/-}Arf^{+/+}$ cells also exhibited a dysregulated cell cycle profile evidenced by marked decrease in the proportion of cells in G1 phase and increase in the proportion in G2/M phase (Figure 1b). Introduction of p16 expression in $p16^{-/-}Arf^{+/+}$ cells normalized the cell cycle distribution, increasing the fraction of cells in G1 phase and decreasing the fraction in G2/M phase (Figure 1b). These results provide evidence that expression of p16 is both necessary and sufficient in $p16^{-/-}Arf^{+/+}$ cells to mediate oxidative and cell-cycle regulation.

In some experimental systems, p16 expression was associated with both senescence and increased ROS (Takahashi *et al.*, 2006), while in others increased p16 expression was not associated with increased ROS (Macip *et al.*, 2002). Thus we examined whether reduced ROS associated with introduction of p16 into $p16^{-/-}Arf^{+/+}$ cells was associated with cellular senescence. The $p16^{-/-}Arf^{+/+}$ fibroblasts were separately infected with either lentivirus expressing p16/GFP or GFP alone, and then assessed for β-galactosidase (β-gal) activity over a 7-day period. We found that while no senescent cells were evident in cultures of $p16^{-/-}Arf^{+/+}$ fibroblasts infected with control GFP lentivirus, cells infected with p16 lentivirus became increasingly positive for senescence-associated β-gal (Supplementary Figure S1). Thus although the relationship between p16 expression and ROS appears subject to experimental context (Vurusaner *et al.*, 2012), in our system restoring p16 expression correlates with reduced ROS and increased G1 arrest and senescence.

Functional activities of familial melanoma-associated p16 mutants

To investigate the potential functional consequences of particular mutations in p16 that have been identified in human melanoma kindreds (Becker *et al.*, 2001; Hashemi *et al.*, 2000; Kannengiesser *et al.*, 2009; McKenzie *et al.*, 2010), we prepared lentiviral constructs encoding 12 point mutants spanning the length of the p16 coding region (Supplementary Table S1). While nine of the mutations are predicted to affect only the p16 and not Arf coding sequences (R24P, R24Q, G35A, G35V, A36P, A57V, L97R, R99P, V126D), the remaining three mutations are predicted to affect both p16 and Arf (P81T, R87W, P114S). Each mutant was separately expressed in $p16^{-/-}Arf^{+/+}$ fibroblasts, and levels of ROS and cell cycle distribution were determined and compared to that of cells expressing either GFP or wild-type p16. Please refer to Table I for a guide to the functional grouping of these mutants and the relevant figures where the data can be found. We defined “loss of function” mutants as those demonstrating less than 30% restoration of function compared to the wild type protein, as defined previously by others (Kannengiesser *et al.*, 2009). Using this

criterion, we found that several p16 mutants exhibited an impaired capacity to regulate both oxidative stress and the cell cycle. For example, ROS levels and cell cycle distribution remained dysregulated in cells expressing the P81T mutant compared to wild-type p16 (Figure 2a). A similar phenotype was observed with the L97R (Figure 2b), and R87W (Figure 2c) mutants. Thus three of the 12 mutants could be categorized as "double loss of function" (Figure 3).

Interestingly, several p16 mutants largely restored regulation of both oxidative stress and cell cycle distribution. For example, expression of the G35A mutant resulted in ROS levels and cell cycle distribution that was more comparable to that of cells expressing wild-type p16 than GFP (Figure 2d, Supplementary Figure S3). A similar phenotype was observed for the R24P (Supplementary Figure S2) and G35V (Supplementary Figure S3) mutants. In some cases, because the replicates were very close, we achieved statistically significant differences between mutant and WT with respect to cell cycle parameters, although the mutant's activity clearly resembled WT more than GFP. This was the case with the A57V mutant (Figure 2a), as well as G35A (Figures 2d, S3), R24P (Figure S2), and G35V (Figure S3). The identification of these three mutants (none of which affect Arf) that largely retain both oxidative and cell cycle regulatory functions (Figure 3) suggests that some mutations in p16 may affect melanoma predisposition by disrupting other (yet undefined) functional activities.

Uncoupling of cell cycle and oxidative regulatory functions

For the remaining six p16 mutants, we found that the oxidative or cell cycle regulatory activity was selectively compromised. For example, the A57V mutant normalized cell-cycle distribution comparable to wild-type p16, but did not correct elevated ROS levels (Figure 2a). Similarly, the A36P (Figure 2b) and P114S mutants (Figure 2c) demonstrated selective loss of oxidative compared to cell cycle regulation. The inverse result was observed with the R99P mutant, which effectively suppressed ROS levels but did not restore cell-cycle distribution (Figure 2d, Supplementary Figure S4). Similarly, selective loss of cell cycle compared to oxidative regulatory function was observed in the V126D (Supplementary Figure S2) and R24Q (Supplementary Figure S4) mutants. Thus the identification of these six mutants in which the oxidative and cell cycle regulatory functions are relatively uncoupled (Figure 3) supports our previous contention that p16 regulates oxidative stress in a cell cycle-independent manner (Jenkins *et al.*, 2011).

p16 mutants with altered functional activities retain appropriate subcellular localization

It is thought that p16 localizes to the nucleus to exert its CDK-inhibitory function (Bartkova *et al.*, 1996; Lukas *et al.*, 1995), although exogenous over-expression of p16 can lead to protein aggregation in the cytoplasm and loss of function (Tevelev *et al.*, 1996). It has also been suggested that cytoplasmic localization of p16 may represent a specific mechanism of its inactivation in tumors (Evangelou *et al.*, 2004). To demonstrate that alterations in functional activities of some p16 mutants were not due to protein mislocalization, we assessed their subcellular localization in $p16^{-/-}Arf^{+/+}$ fibroblasts by immunofluorescence. First, we confirmed that wild-type p16 was strongly nuclear, and no cytosolic expression was detected (Supplementary Figure S5). Analysis of the 12 different point mutants

consistently showed similar nuclear localization (Supplementary Figure S5), suggesting that their various altered functional activities could not be attributed to p16 mislocalization.

Analysis of p16-regulatory functions in human melanoma cells

Next, we examined a subset of these mutants in human melanoma cells – perhaps a more relevant model for analyzing p16 mutations associated with familial melanoma. WM793 cells that do not express p16 were transduced with lentivirus expressing either GFP, wild-type p16, or a selected p16 mutant. As above, we optimized expression of individual mutants to be comparable to expression levels of wild-type p16 (Figure 4a, b). As observed in p16-deficient mouse fibroblasts (Figure 1), expression of wild-type p16 was associated both with ROS suppression (Figure 4c, d) and cell cycle shift (Figure 4e, f). Mirroring the phenotypes seen above (Figure 2c, d), the R99P mutant retained oxidative but not cell cycle function while the P114S mutant exhibited the reciprocal phenotype (Figure 4c, e) in WM793 cells. Compared to wild-type p16, the R24Q mutant was unable to restore significant oxidative (Figure 4d) or cell cycle function (Figure 4f) consistent with earlier findings (Supplementary Figure S4). Finally, as seen above (Supplementary Figure S3), the G35V mutant retained cell cycle function comparable to wild-type p16 (Figure 4f), and exhibited intermediate capacity for reducing ROS (Figure 4d). Importantly, the differential capacity of three p16 mutants (R99P, P114S, G35V) to regulate oxidative versus cell cycle regulatory functions was recapitulated in human melanoma cells.

Structure-function relationships among p16 mutants

Finally, we examined relative localization of these mutations based on published structures of the molecule (Byeon *et al.*, 1998; Russo *et al.*, 1998). p16 consists mainly of four ankyrin repeats, a conserved motif involved in various protein-protein interactions (Li *et al.*, 2006). While some studies have implicated all four ankyrin repeats as important for CDK4/6-binding and cell cycle inhibition, others indicate that the third ankyrin repeat (residues 81–113) as well as the β-hairpin loop within the second ankyrin repeat (residues 52–54) are the most critical regions for mediating these functions (Byeon *et al.*, 1998; Mahajan *et al.*, 2007; Russo *et al.*, 1998). Consistent with this notion, several residues that we found to be important for both cell-cycle and oxidative regulation (P81, R87, L97), or only cell-cycle regulation (R99), reside in the third ankyrin repeat (Supplementary Figure S6). By contrast, most residues important for oxidative but not cell-cycle regulation (A36, A57, P114), or those not important for either function (G35, R24), are not found within the third ankyrin repeat or the β-hairpin loop of the second ankyrin repeat (Supplementary Figure S6).

DISCUSSION

We recently described a role for p16 in suppressing intracellular oxidative stress, functioning independently of cell cycle and its control of the Rb pathway (Jenkins *et al.*, 2011). These two regulatory functions are likely to be complementary in preventing potentially oncogenic oxidative DNA lesions by decreasing their formation (reduction of ROS) and propagation (induction of cell cycle arrest to allow DNA repair). In this study we examined separately the cell cycle and oxidative regulatory capacities of a panel of familial melanoma-associated p16 point mutants. In half of these mutants, one of these two activities

was selectively compromised (Figure 3). These findings provide further evidence that p16 regulates intracellular oxidative stress independently of the cell-cycle.

Historically, the cell cycle regulatory function of familial p16 mutants was assessed by measuring CDK4-binding – since p16 binding to CDK4/6 is the critical step leading to reduction in Rb phosphorylation and inhibition of the G1/S transition (Alcorta *et al.*, 1996; Lukas *et al.*, 1995). The two primary assays employed were based on yeast two-hybrid (Yang *et al.*, 1995) and immunoprecipitation (Becker *et al.*, 2001; Hashemi *et al.*, 2000; Kannengiesser *et al.*, 2009), which, have been problematic for two reasons. First, several mutants retained the capacity to bind CDK4, yet were greatly reduced in capacity for cell cycle regulation (Becker *et al.*, 2001; Koh *et al.*, 1995). These discrepancies could reflect the additional known capacity of p16 to bind CDK6 and intact CDK4/6-cyclinD complexes in addition to CDK4 (Hirai *et al.*, 1995; Serrano *et al.*, 1993), neither of which was measured in past studies. Differences in functional assays may also relate to the potential ability of p16 to bind and inhibit CDK7, a kinase subunit of the TFIIH transcription factor (Serizawa 1998), which may allow induction of cell cycle arrest independently of CDK4/6-binding (Nishiwaki *et al.*, 2000). In addition to lack of correlation between CDK4-binding and cell-cycle inhibitory functions found in some cases, other studies have reported differences in CDK4-binding activity for the same p16 mutant. For example, the reported CDK4-binding activity of the G101W mutant ranged from 5 to 73% of wild-type, based on yeast two-hybrid (Reymond and Brent 1995; Yang *et al.*, 1995) and immunoprecipitation assays (Becker *et al.*, 2001; Parry and Peters 1996; Ranade *et al.*, 1995; Walker *et al.*, 1995). A mammalian two-hybrid assay has also been used to measure interactions between p16 mutants and CDK4 in human osteosarcoma (Saos-2) cells (McKenzie *et al.*, 2010). While mammalian cells allow for post-translational modifications, there could be important differences between these tumor cells and melanocytes or melanoma cells. Rather than developing our own assay based on CDK4-, CDK6- or CDK4/6-cyclin D binding, we wanted to avoid these pitfalls and directly measure cell-cycle regulatory activity; thus we determined cell-cycle distribution by flow cytometry (which was highly reproducible) as a readout of the cell-cycle regulatory function of these p16 mutants.

Several previous studies have characterized the effect of p16 point mutations on cell cycle regulatory activity, yielding a wide range of phenotypes among different mutants and conflicting results concerning the same mutants. Some discrepancies may lie in the different assays and cell types used for assessing cell cycle function, which included ability to induce phase arrest (Becker *et al.*, 2001; Becker *et al.*, 2005; Koh *et al.*, 1995; McKenzie *et al.*, 2010; Miller *et al.*, 2011), limit cell numbers in culture (Jones *et al.*, 2007; Kannengiesser *et al.*, 2009), reduce proliferation by Ki67/BrdU staining (Jones *et al.*, 2007; McKenzie *et al.*, 2010), and reduce colony formation (Becker *et al.*, 2005; Jones *et al.*, 2007) in fibroblasts, osteosarcoma, and melanoma cells. For the mutants studied here, however, our results largely agreed with that reported in the literature. For example, our observations that cell cycle function was retained (R24P, G35A, G35V) or only partially diminished (A36P, A57V, P114S) in these particular mutants is consistent with prior reports (Jones *et al.*, 2007; Kannengiesser *et al.*, 2009; McKenzie *et al.*, 2010). Similarly, our findings that cell cycle function was largely diminished (V126D) or completely absent (R99P, R87W, L97R) in

other mutants is consistent with previous studies (Becker *et al.*, 2001; Kannengiesser *et al.*, 2009; McKenzie *et al.*, 2010; Miller *et al.*, 2011). On the other hand, the lack of cell cycle regulatory function that we observed for mutants R24Q and P81T was not consistent with earlier studies in which the R24Q (Kannengiesser *et al.*, 2009) and P81T (McKenzie *et al.*, 2010) mutants were found to be comparable to wild-type p16. For the R24Q mutant, we confirmed lack of cell cycle function in WM793 human melanoma cells (Figure 4f). As suggested above, one explanation for these discrepancies in addition to the different assays use of different cell types. The capacity of some mutants to regulate cell cycle may be unmasked in particular cellular contexts depending on the different interactions of p16 (i.e. with various CDKs) that could be affected. In addition, some cell lines may be less susceptible to regulation by exogenous p16 due to the presence of background mutations, or loss of the entire *CDKN2A* locus with corresponding lack of dependency on p16 or ARF.

It has been reported that the third ankyrin repeat of p16 (residues 81–113) and a β-hairpin loop in the second ankyrin repeat (residues 52–54) are the most important regions for CDK4-binding (Byeon *et al.*, 1998; Fahraeus *et al.*, 1996; Li *et al.*, 1999; Mahajan *et al.*, 2007). Our results further confirm the importance of this region in p16 for cell cycle regulation, as the R99P mutant which demonstrates the most dramatic loss of cell cycle function while retaining oxidative function (Figure 3) is located in the third ankyrin repeat (Supplementary Figure S6). This region forms both an extensive hydrogen-bond network at the interface of CDK4/6 (involving residues 74, 84, and 87 of p16) and a mostly hydrophobic structural core that interacts with the other internal helices that may help stabilize the protein (Russo *et al.*, 1998). Perhaps several mutations in this region upset either the hydrogen bond network of the binding interface or these internal stabilizing helices, as most mutants that fail to restore both cell cycle and oxidative regulatory function (P81T, R87W, L97R) are located here (Supplementary Figure S6). Consistent with this notion, the mutants that failed to impair either function (R24P, G35A, G35V), or that selectively impaired oxidative regulation (A36P, A57V, P114S), are located outside of this region. These residues may be involved in direct or indirect interactions with yet uncharacterized binding partners of p16, or mutations of these residues could alter the secondary structure of the p16 molecule that precludes interactions required for oxidative regulatory function. The potential effects of particular mutations studied here on p16 structure are difficult to predict without analysis of crystal structures of the mutant p16 molecules.

The identification of several familial melanoma-associated mutants that largely retain both regulatory functions (Figure 3) suggests that some p16 mutations may affect melanoma predisposition by disrupting some other yet-to-be defined tumor-suppressor function. There is precedent for other well-studied tumor suppressor genes that appear to regulate ROS independently of their canonical functions (Vurusaner *et al.*, 2012). For example, p53 is a regulator of ROS as several p53-target genes include redox-active proteins and ROS-generating enzymes (Macip *et al.*, 2003; Polyak *et al.*, 1997), and many post-translational modifications of p53 generate ROS (Bragado *et al.*, 2007). Another example is the CDK inhibitor p21 that regulates oxidative stress by increasing stability of Nrf2, allowing increased Nrf2-mediated transactivation of several antioxidant enzymes (Chen *et al.*, 2009).

Finally, the breast cancer susceptibility genes BRCA1 and BRCA2 also appear involved in regulating oxidative stress. BRCA1 upregulates multiple antioxidant genes, including glutathione S-transferases and oxidoreductases (Bae *et al.*, 2004), and both BRCA1 and BRCA2 are required for repair of the oxidative DNA lesion 8-oxoguanine (Le Page *et al.*, 2000). The elucidation of non-canonical roles of p16 as well as these other tumor suppressors in the regulation of cellular oxidative stress may signal the development of a new paradigm in which tumor-suppressor proteins employ multiple mechanisms that may be disabled in cancer, or in patients with cancer predisposition syndromes.

MATERIALS AND METHODS

Cell culture

Murine fibroblasts were isolated from newborn wild-type (FVB) and background-matched $p16^{-/-}Arf^{+/+}$ (#01XE4, FVB.129-*Cdkn2a*$^{tm2.1Rdp}$) homozygous mice (Kamijo *et al.*, 1997), both obtained from the National Cancer Institute (Rockville, MD, USA), as we have previously described (Jenkins *et al.*, 2011). These procedures were approved by the University of Utah IACUC. Early passage cells (approximately two weeks after isolation) were aliquotted and stored at −80 °C. For each set of experiments, fresh cells were thawed and used over a 2–3 week period. WM793 melanoma cells were originally obtained from Meenhard Herlyn (Wistar Institute, Philadelphia, PA, USA).

Western blotting

Specific proteins were detected in cell lysates by Western blotting as previously described (Jenkins *et al.*, 2011). Primary antibodies were used against p16 (1:1000, Santa Cruz Biotechnology, Santa Cruz, CA, USA), β-actin (1:10 000, A-3853, Sigma-Aldrich, St. Louis, MO, USA), and ARF (1:1000, sc-22784, Santa Cruz Biotechnology).

Measurement of oxidative stress

Endogenous ROS of protein equivalents (30 μg) were quantified using 2,7-dichlorodihydrofluorescein diacetate (DCFDA, Life Technologies, Grand Island, NY, USA) as previously described (Jenkins *et al.*, 2011). All experiments were performed in triplicate.

p16-expressing lentiviruses

The lentivirus expressing human wild-type p16 is previously described (Jenkins *et al.*, 2011). The p16 point mutant constructs were generated by PCR-based segment overlap as described previously (Raj *et al.*, 2008), using human p16 cDNA as a template and primers designed to create specific point mutations. Briefly, an initial PCR reaction was used to separately create the 5′ and 3′ fragments for each mutant. The 5′ fragment was constructed using wild-type p16 sequence as “primer 1” and mutant sequence as “primer 2”, and the 3′ fragment was constructed using wild-type p16 sequence as “primer 2” and mutant sequence as “primer 1” (see Supplemental text, Table S1). A second PCR reaction was then used to anneal these individual segments, using equimolar amounts of the 5′ and 3′ fragments as template and primers corresponding to wild-type p16. The final PCR product was cloned into a modified pHIV-Zsgreen (Addgene #18121) lentiviral expression vector (Welm *et al.*, 2008) and confirmed by DNA sequencing. Each lentiviral construct was validated for p16

expression by transient transfection into HeLa cells followed by western blotting. Viruses were produced in HEK 293T/17 cells (ATCC, Manassas, VA, USA) co-transfected with 5 μg lentiviral vector and 1.7 μg of each helper plasmid (pRSV-REV, pMDLg/pRRE and pVSVG, generously provided by Brian Welm, Huntsman Cancer Institute) and 30 μg of polyethylenimine (pH 7.0, Sigma) in 1 mL of OptiMEM (Life Technologies). Viral particles were collected, purified, concentrated, titered, and stored as described previously (Jenkins *et al.*, 2011). For cellular infection, 8 μg per mL polybrene (Sigma) was added. Assays for oxidative stress and cell cycle distribution in WM793 cells were performed 16 h and 48 h after infection, respectively, and after 72 h in fibroblasts. Experiments involving each mutant were performed at least twice.

Cell cycle analysis

Cells were harvested by trypsinization, washed, fixed, stained with 50 mg per mL propidium iodide (Sigma), and analyzed as described previously (Jenkins *et al.*, 2011). All experiments were performed in triplicate.

Senescence-associated β-gal staining

Staining was performed as described previously (Cotter *et al.*, 2007). Briefly, cells were fixed in 1% paraformaldehyde and then stained overnight at 37°C in a solution (pH 6.0) containing potassium ferrocyanide, potassium ferricyanide, and 5-bromo-4-chloro-3-indolyl-b-D-galactoside (X-gal). All experiments were performed in triplicate.

Immunofluorescence

Cultured fibroblasts were seeded on coverslips in 12-well plates at 30–40% confluency, tranduced by lentivirus, and then fixed 72 h post-infection with PBS containing 4 % paraformaldehyde for 15 min. Cells were permeabilized with 0.2 %Triton X-100 in PBS, then immunostained for 60 min with anti-p16 (1:1000, sc-1661, Santa Cruz Biotechnology), followed by a 60 min exposure to Alexa Fluor 594-conjugated secondary IgG (1:200, A-11062, Life Technologies). Images were captured on a Zeiss Axioskop2 automated microscope, using an Axio Cam MRm camera and AxioVision 4.8.1 software (Carl Zeiss Microscopy, Thornwood, NY, USA), and then processed with ImageJ software (http://rsbweb.nih.gov/ij/download.html).

Structural Analysis

Structural modeling of p16 was performed using SwissPdb Viewer (http://www.expasy.org/spdbv) as described elsewhere (Guex and Peitsch 1997), based on the p16 published structure 1a5e (Byeon *et al.*, 1998).

Statistics

Analyses were performed with Prism 3.0 software (GraphPad). Data derived from multiple determinations were subjected to two-sided *t* tests. P values ≤ 0.05 were considered statistically significant. Statistical significance is denoted within each figure by asterisks with *, **, and *** indicating P values of ≤0.05, ≤0.01, and ≤0.001, respectively.

Supplementary Material

Refer to Web version on PubMed Central for supplementary material.

Acknowledgments

We thank Meenhard Herlyn for the WM793 cells, and Bryan Welm for the lentiviral helper plasmids. This work was supported in part by a U of U seed grant, the Department of Dermatology, and the Huntsman Cancer Foundation. We acknowledge use of the DNA/peptide and Flow cytometry core facilities supported by P30 CA042014 awarded to Huntsman Cancer Institute. M.W. was supported by grant T35 HL007744. We thank Sancy Leachman for critically reviewing an earlier version of the manuscript.

Abbreviations

Arf	Alternative reading frame
β-gal	β-galactosidase
CDK	cyclin-dependent kinase
GFP	green fluorescent protein
ROS	reactive oxygen species

References

Alcorta DA, Xiong Y, Phelps D, Hannon G, Beach D, Barrett JC. Involvement of the cyclin-dependent kinase inhibitor p16 (INK4a) in replicative senescence of normal human fibroblasts. Proc Natl Acad Sci U S A. 1996; 93:13742–7. [PubMed: 8943005]

Bae I, Fan S, Meng Q, Rih JK, Kim HJ, Kang HJ, et al. BRCA1 induces antioxidant gene expression and resistance to oxidative stress. Cancer Res. 2004; 64:7893–909. [PubMed: 15520196]

Bartkova J, Lukas J, Guldberg P, Alsner J, Kirkin AF, Zeuthen J, et al. The p16-cyclin D/Cdk4-pRb pathway as a functional unit frequently altered in melanoma pathogenesis. Cancer Res. 1996; 56:5475–83. [PubMed: 8968104]

Becker TM, Rizos H, Kefford RF, Mann GJ. Functional impairment of melanoma-associated p16(INK4a) mutants in melanoma cells despite retention of cyclin-dependent kinase 4 binding. Clin Cancer Res. 2001; 7:3282–8. [PubMed: 11595726]

Becker TM, Ayub AL, Kefford RF, Mann GJ, Rizos H. The melanoma-associated 24 base pair duplication in p16INK4a is functionally impaired. Int J Cancer. 2005; 117:569–73. [PubMed: 15945100]

Bishop DT, Demenais F, Goldstein AM, Bergman W, Bishop JN, Bressac-de Paillerets B, et al. Geographical variation in the penetrance of CDKN2A mutations for melanoma. J Natl Cancer Inst. 2002; 94:894–903. [PubMed: 12072543]

Bragado P, Armesilla A, Silva A, Porras A. Apoptosis by cisplatin requires p53 mediated p38alpha MAPK activation through ROS generation. Apoptosis. 2007; 12:1733–42. [PubMed: 17505786]

Byeon IJ, Li J, Ericson K, Selby TL, Tevelev A, Kim HJ, et al. Tumor suppressor p16INK4A: determination of solution structure and analyses of its interaction with cyclin-dependent kinase 4. Mol Cell. 1998; 1:421–31. [PubMed: 9660926]

Chen W, Sun Z, Wang XJ, Jiang T, Huang Z, Fang D, et al. Direct interaction between Nrf2 and p21(Cip1/WAF1) upregulates the Nrf2-mediated antioxidant response. Mol Cell. 2009; 34 :663–73. [PubMed: 19560419]

Cotter MA, Florell SR, Leachman SA, Grossman D. Absence of senescence-associated beta-galactosidase activity in human melanocytic nevi in vivo. J Invest Dermatol. 2007; 127:2469–71. [PubMed: 17522702]

Evangelou K, Bramis J, Peros I, Zacharatos P, Dasiou-Plakida D, Kalogeropoulos N, et al. Electron microscopy evidence that cytoplasmic localization of the p16(INK4A) “nuclear” cyclin-dependent kinase inhibitor (CKI) in tumor cells is specific and not an artifact. A study in non-small cell lung carcinomas. Biotech Histochem. 2004; 79:5–10. [PubMed: 15223748]

Fahraeus R, Paramio JM, Ball KL, Lain S, Lane DP. Inhibition of pRb phosphorylation and cell-cycle progression by a 20-residue peptide derived from p16CDKN2/INK4A. Curr Biol. 1996; 6:84–91. [PubMed: 8805225]

Goldstein AM, Chan M, Harland M, Hayward NK, Demenais F, Bishop DT, et al. Features associated with germline CDKN2A mutations: a GenoMEL study of melanoma-prone families from three continents. J Med Genet. 2007; 44:99–106. [PubMed: 16905682]

Guex N, Peitsch MC. SWISS-MODEL and the Swiss-PdbViewer: an environment for comparative protein modeling. Electrophoresis. 1997; 18:2714–23. [PubMed: 9504803]

Hashemi J, Platz A, Ueno T, Stierner U, Ringborg U, Hansson J. CDKN2A germ-line mutations in individuals with multiple cutaneous melanomas. Cancer Res. 2000; 60:6864–7. [PubMed: 11156381]

Herrling T, Jung K, Fuchs J. Measurements of UV-generated free radicals/reactive oxygen species (ROS) in skin. Spectrochim Acta A Mol Biomol Spectrosc. 2006; 63:840–5. [PubMed: 16543118]

Hirai H, Roussel MF, Kato JY, Ashmun RA, Sherr CJ. Novel INK4 proteins, p19 and p18, are specific inhibitors of the cyclin D-dependent kinases CDK4 and CDK6. Mol Cell Biol. 1995; 15 :2672–81. [PubMed: 7739547]

Jenkins NC, Liu T, Cassidy P, Leachman SA, Boucher KM, Goodson AG, et al. The p16(INK4A) tumor suppressor regulates cellular oxidative stress. Oncogene. 2011; 30:265–74. [PubMed: 20838381]

Jones R, Ruas M, Gregory F, Moulin S, Delia D, Manoukian S, et al. A CDKN2A mutation in familial melanoma that abrogates binding of p16INK4a to CDK4 but not CDK6. Cancer Res. 2007; 67:9134–41. [PubMed: 17909018]

Kamijo T, Zindy F, Roussel MF, Quelle DE, Downing JR, Ashmun RA, et al. Tumor suppression at the mouse INK4a locus mediated by the alternative reading frame product p19ARF. Cell. 1997; 91:649–59. [PubMed: 9393858]

Kannengiesser C, Brookes S, del Arroyo AG, Pham D, Bombled J, Barrois M, et al. Functional, structural, and genetic evaluation of 20 CDKN2A germ line mutations identified in melanoma-prone families or patients. Hum Mutat. 2009; 30:564–74. [PubMed: 19260062]

Koh J, Enders GH, Dynlacht BD, Harlow E. Tumour-derived p16 alleles encoding proteins defective in cell-cycle inhibition. Nature. 1995; 375:506–10. [PubMed: 7777061]

Le Page F, Randrianarison V, Marot D, Cabannes J, Perricaudet M, Feunteun J, et al. BRCA1 and BRCA2 are necessary for the transcription-coupled repair of the oxidative 8-oxoguanine lesion in human cells. Cancer Res. 2000; 60:5548–52. [PubMed: 11034101]

Li J, Byeon IJ, Ericson K, Poi MJ, O’Maille P, Selby T, et al. Tumor suppressor INK4: determination of the solution structure of p18INK4C and demonstration of the functional significance of loops in p18INK4C and p16INK4A. Biochemistry. 1999; 38:2930–40. [PubMed: 10074345]

Li J, Mahajan A, Tsai MD. Ankyrin repeat: a unique motif mediating protein-protein interactions. Biochemistry. 2006; 45:15168–78. [PubMed: 17176038]

Lukas J, Parry D, Aagaard L, Mann DJ, Bartkova J, Strauss M, et al. Retinoblastoma-protein-dependent cell-cycle inhibition by the tumour suppressor p16. Nature. 1995; 375:503–6. [PubMed: 7777060]

Macip S, Igarashi M, Fang L, Chen A, Pan ZQ, Lee SW, et al. Inhibition of p21-mediated ROS accumulation can rescue p21-induced senescence. EMBO J. 2002; 21:2180–8. [PubMed: 11980715]

Macip S, Igarashi M, Berggren P, Yu J, Lee SW, Aaronson SA. Influence of induced reactive oxygen species in p53-mediated cell fate decisions. Mol Cell Biol. 2003; 23:8576–85. [PubMed: 14612402]

Mahajan A, Guo Y, Yuan C, Weghorst CM, Tsai MD, Li J. Dissection of protein-protein interaction and CDK4 inhibition in the oncogenic versus tumor suppressing functions of gankyrin and P16. J Mol Biol. 2007; 373:990–1005. [PubMed: 17881001]

McKenzie HA, Fung C, Becker TM, Irvine M, Mann GJ, Kefford RF, et al. Predicting functional significance of cancer-associated p16(INK4a) mutations in CDKN2A. Hum Mutat. 2010; 31 :692–701. [PubMed: 20340136]

Miller PJ, Duraisamy S, Newell JA, Chan PA, Tie MM, Rogers AE, et al. Classifying variants of CDKN2A using computational and laboratory studies. Hum Mutat. 2011; 32:900–11. [PubMed: 21462282]

Nishiwaki E, Turner SL, Harju S, Miyazaki S, Kashiwagi M, Koh J, et al. Regulation of CDK7-carboxyl-terminal domain kinase activity by the tumor suppressor p16(INK4A) contributes to cell cycle regulation. Mol Cell Biol. 2000; 20:7726–34. [PubMed: 11003668]

Parry D, Peters G. Temperature-sensitive mutants of p16CDKN2 associated with familial melanoma. Mol Cell Biol. 1996; 16:3844–52. [PubMed: 8668202]

Polyak K, Xia Y, Zweier JL, Kinzler KW, Vogelstein B. A model for p53-induced apoptosis. Nature. 1997; 389:300–5. [PubMed: 9305847]

Raj D, Liu T, Samadashwily G, Li F, Grossman D. Survivin repression by p53, Rb and E2F2 in normal human melanocytes. Carcinogenesis. 2008; 29:194–201. [PubMed: 17916908]

Ranade K, Hussussian CJ, Sikorski RS, Varmus HE, Goldstein AM, Tucker MA, et al. Mutations associated with familial melanoma impair p16INK4 function. Nat Genet. 1995; 10:114–6. [PubMed: 7647780]

Reymond A, Brent R. p16 proteins from melanoma-prone families are deficient in binding to Cdk4. Oncogene. 1995; 11:1173–8. [PubMed: 7566978]

Russo AA, Tong L, Lee JO, Jeffrey PD, Pavletich NP. Structural basis for inhibition of the cyclin-dependent kinase Cdk6 by the tumour suppressor p16INK4a. Nature. 1998; 395:237–43. [PubMed: 9751050]

Serizawa H. Cyclin-dependent kinase inhibitor p16INK4A inhibits phosphorylation of RNA polymerase II by general transcription factor TFIIH. J Biol Chem. 1998; 273:5427–30. [PubMed: 9488660]

Serrano M, Hannon GJ, Beach D. A new regulatory motif in cell-cycle control causing specific inhibition of cyclin D/CDK4. Nature. 1993; 366:704–7. [PubMed: 8259215]

Shapiro GI, Edwards CD, Ewen ME, Rollins BJ. p16INK4A participates in a G1 arrest checkpoint in response to DNA damage. Mol Cell Biol. 1998; 18:378–87. [PubMed: 9418885]

Sharpless NE, DePinho RA. The INK4A/ARF locus and its two gene products. Curr Opin Genet Dev. 1999; 9:22–30. [PubMed: 10072356]

Takahashi A, Ohtani N, Yamakoshi K, Iida S, Tahara H, Nakayama K, et al. Mitogenic signalling and the p16INK4a-Rb pathway cooperate to enforce irreversible cellular senescence. Nat Cell Biol. 2006; 8:1291–7. [PubMed: 17028578]

Tevelev A, Byeon IJ, Selby T, Ericson K, Kim HJ, Kraynov V, et al. Tumor suppressor p16INK4A: structural characterization of wild-type and mutant proteins by NMR and circular dichroism. Biochemistry. 1996; 35:9475–87. [PubMed: 8755727]

Vurusaner B, Poli G, Basaga H. Tumor suppressor genes and ROS: complex networks of interactions. Free Radic Biol Med. 2012; 52:7–18. [PubMed: 22019631]

Walker GJ, Hussussian CJ, Flores JF, Glendening JM, Haluska FG, Dracopoli NC, et al. Mutations of the CDKN2/p16INK4 gene in Australian melanoma kindreds. Hum Mol Genet. 1995; 4:1845–52. [PubMed: 8595405]

Welm BE, Dijkgraaf GJ, Bledau AS, Welm AL, Werb Z. Lentiviral transduction of mammary stem cells for analysis of gene function during development and cancer. Cell Stem Cell. 2008; 2:90–102. [PubMed: 18371425]

Yang R, Gombart AF, Serrano M, Koeffler HP. Mutational effects on the p16INK4a tumor suppressor protein. Cancer Res. 1995; 55:2503–6. [PubMed: 7780957]

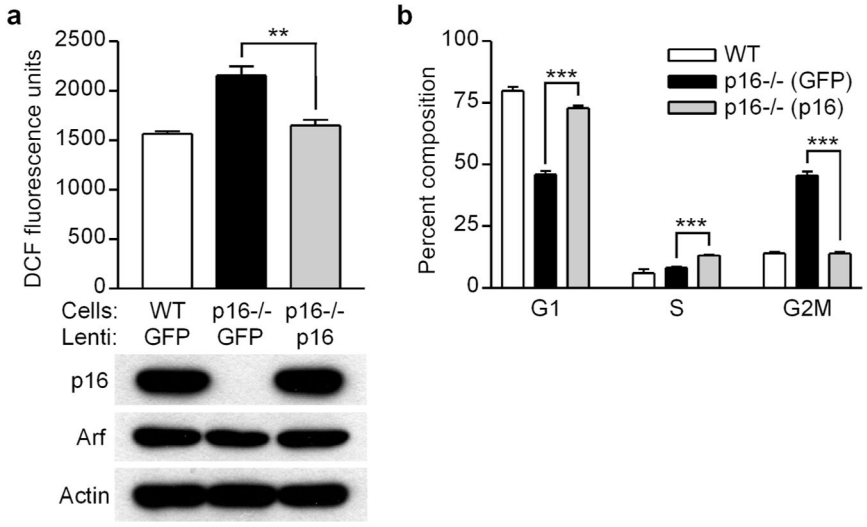

Figure 1. p16 expression normalizes ROS and cell-cycle profile in $p16^{-/-}Arf^{+/+}$ cells

(**a**) Wild-type (WT) and *p16*-deficient fibroblasts were infected with either GFP (control) lentivirus or lentivirus expressing wild-type p16 as indicated. After 72 h, cell lysates were subjected to DCFDA assay for intracellular ROS (upper panel) and western blotting for p16, Arf, or actin (lower panel). Error bars indicate SEM from triplicate determinations, **P≤0.01. (**b**) After 72 h, cell cycle analysis was performed with percentages of cells in each phase (G1, S, G2M) indicated. Error bars indicate SEM from triplicate determinations, ***P ≤0.001.

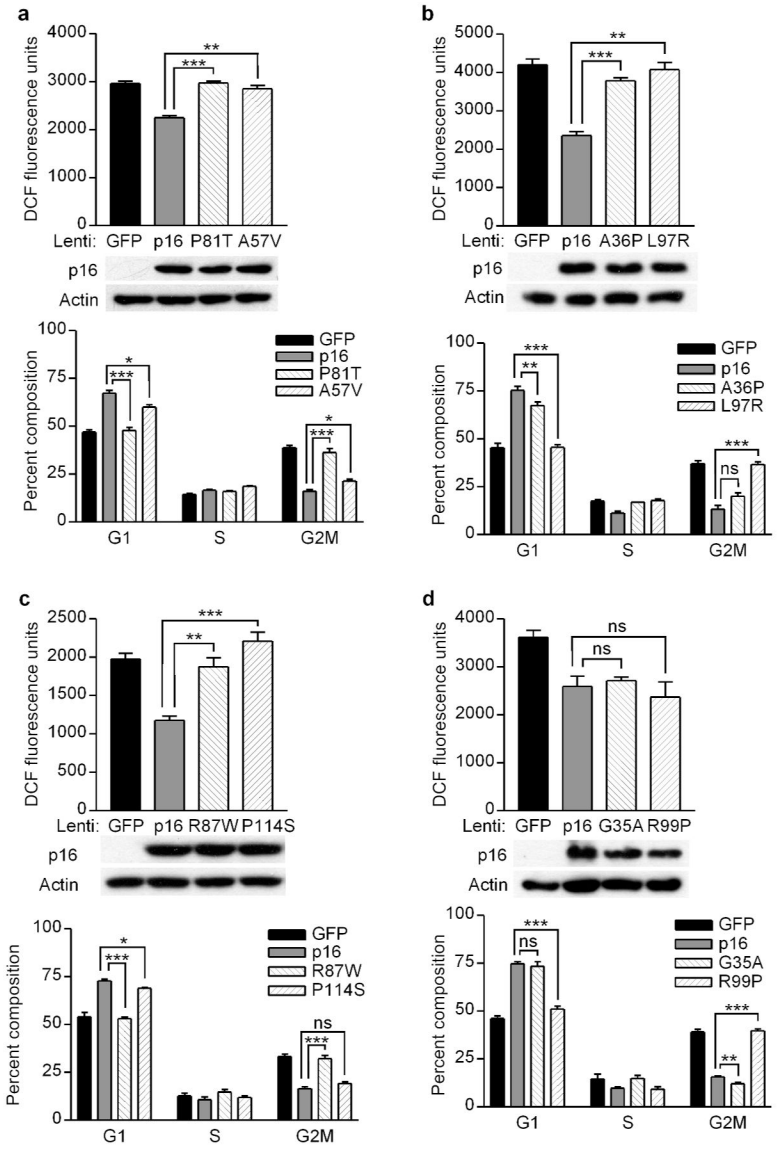

Figure 2. Functional activities of familial melanoma-associated p16 mutants

p16-deficient fibroblasts were infected with the indicated lentiviral constructs expressing GFP, wild-type p16, or (**a**) mutants P81T or A57V, (**b**) mutants A36P or L97R, (**c**) mutants R87W or P114S, or (**d**) mutants G35A or R99P. Cell lysates were prepared for detection of ROS and p16 protein levels (upper panels in each). Cell cycle analysis was performed with percentages of cells in each phase (G1, S, G2M) indicated (lower panels in each). Error bars indicate SEM from triplicate determinations. Asterisks *, **, and *** indicate P values of ≤0.05, ≤0.01, and ≤0.001, respectively. ns, not significant.

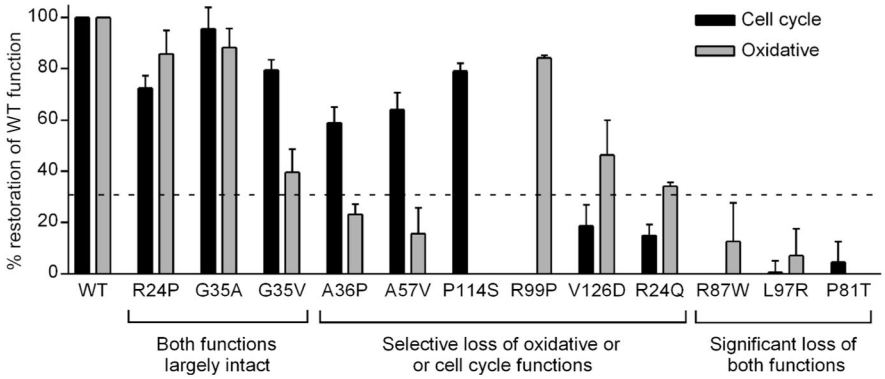

Figure 3. Summary of functional analyses of familial melanoma-associated p16 mutants

Percent restoration (relative to wild-type p16, set at 100%) of cell cycle or oxidative regulatory function is shown after each construct was expressed in p16-deficient fibroblasts. Error bars indicate SEM of triplicate determinations. The cutoff used to categorize a mutant as retaining function was >30% restoration of wild-type function (dashed line).

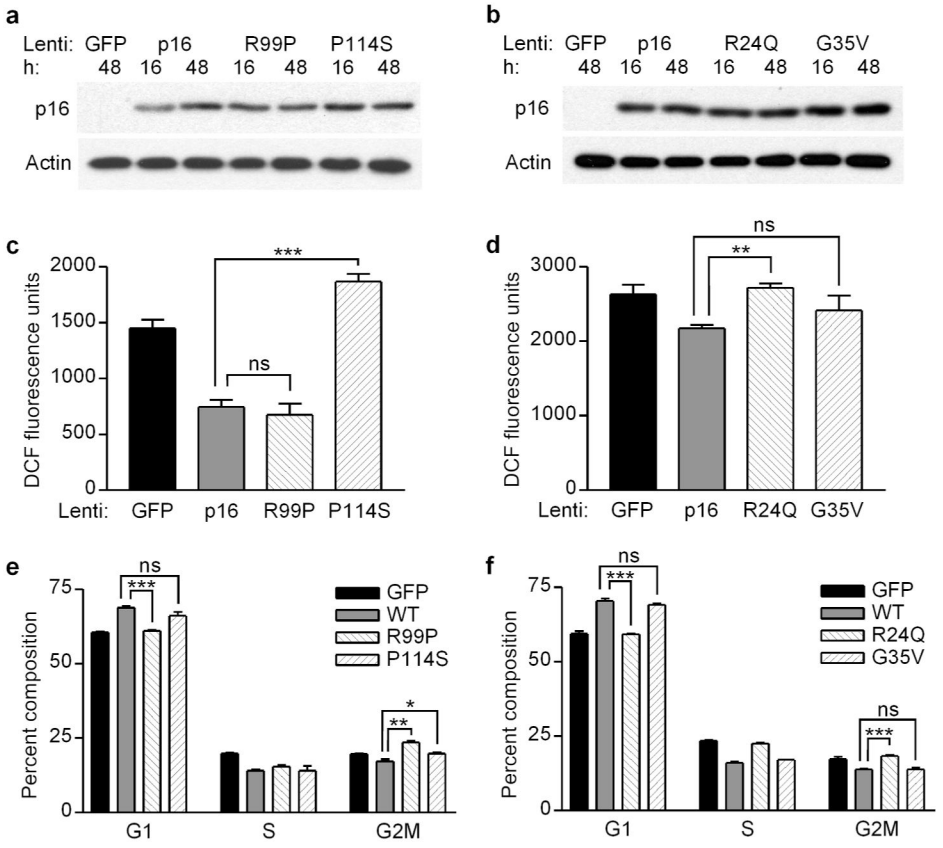

Figure 4. Uncoupling of oxidative and cell cycle regulatory functions by p16 mutants in WM793 human melanoma cells

(**a, b**) WM793 cells were infected with the indicated lentiviral constructs, and cell lysates were collected either 16 h or 48 h post-infection for western blotting. (**c, d**) ROS levels were determined in cell lysates 16 h post-infection with the indicated lentivirus. Error bars indicate SEM from triplicate determinations. Asterisks ** and *** indicate P values of ≤0.01 and ≤0.001, respectively. ns, not significant. (**e, f**) Cell cycle analysis was performed 48 h post-infection with percentages of cells in each phase (G1, S, G2M) indicated. Error bars indicate SEM from triplicate determinations. Asterisks *, **, and *** indicate P values of ≤0.05, ≤0.01, and ≤0.001, respectively. ns, not significant.

TABLE I

Guide to functional activities of p16 mutants

Category	Mutants	Figures
Both functions impaired		
	P81T	2a
	L97R	2b
	R87W	2c
Both functions retained		
	G35A	2d, S3
	R24P	S2
	G35V	S3
Uncoupling of functions		
	A57V	2a
	A36P	2b
	P114S	2c
	R99P	2d, S4
	V126D	S2
	R24Q	S4